

# Price of Anarchy of Traffic Assignment with Exponential Cost Functions

Jianglin Qiao (✉ [30053436@westernsydney.edu.au](mailto:30053436@westernsydney.edu.au))

Western Sydney University

**Dave de Jonge**

Artificial Intelligence Research Institute (IIIA), Spanish Scientific Research Council (CSIC)

**Bo Du**

University of Wollongong

**Dongmo Zhang**

Western Sydney University

**Simeon Simoff**

Western Sydney University

**Carles Sierra**

Artificial Intelligence Research Institute (IIIA), Spanish Scientific Research Council (CSIC)

---

## Research Article

**Keywords:** Price of Anarchy, Congestion Game, Traffic Assignment, Multi-agent System

**Posted Date:** May 9th, 2023

**DOI:** <https://doi.org/10.21203/rs.3.rs-2895881/v1>

**License:**  This work is licensed under a Creative Commons Attribution 4.0 International License.

[Read Full License](#)

**Additional Declarations:** No competing interests reported.

---

**Version of Record:** A version of this preprint was published at Autonomous Agents and Multi-Agent Systems on October 3rd, 2023. See the published version at <https://doi.org/10.1007/s10458-023-09625-6>.

# Price of Anarchy of Traffic Assignment with Exponential Cost Functions

Jianglin Qiao<sup>1,2\*</sup>, Dave de Jonge<sup>2†</sup>, Bo Du<sup>3†</sup>, Dongmo Zhang<sup>1†</sup>,  
Simeon Simoff<sup>1†</sup>, Carles Sierra<sup>2†</sup>

<sup>1</sup>School of Computer, Data and Mathematical Sciences, Western Sydney University, Australia.

<sup>2</sup>Artificial Intelligence Research Institute (IIIA), Spanish Scientific Research Council (CSIC), Spain.

<sup>3</sup>SMART Infrastructure Facility, University of Wollongong, Australia.

\*Corresponding author(s). E-mail(s): [J.Qiao@westernsydney.edu.au](mailto:J.Qiao@westernsydney.edu.au);  
Contributing authors: [davedejonge@iiia.csic.es](mailto:davedejonge@iiia.csic.es); [bdu@uow.edu.au](mailto:bdu@uow.edu.au);  
[D.Zhang@westernsydney.edu.au](mailto:D.Zhang@westernsydney.edu.au); [S.Simoff@westernsydney.edu.au](mailto:S.Simoff@westernsydney.edu.au);  
[sierra@iiia.csic.es](mailto:sierra@iiia.csic.es);

†These authors contributed equally to this work.

## Abstract

The advancement of technologies for autonomous vehicles (AVs) provides great potential for intelligent traffic control and management in the future. The deployment of Vehicle-to-Vehicle (V2V), Vehicle-to-Infrastructure (V2I) and Vehicle-to-Everything (V2X) communications enable traffic control on road segments, intersections or regional road networks with more options, either centralized or decentralized. However, choosing these options is not purely technical but a trade-off between autonomous decision-making and system optimization. One useful quantitative criterion for such a trade-off is the price of anarchy (PoA) of autonomous decision-making. This paper analyses the price of anarchy for road networks with traffic of autonomous vehicles. We model a traffic network as a routing game in which vehicles are selfish agents who choose routes to travel autonomously to minimize travel delays caused by road congestion. Unlike existing research in which the latency function of road congestion was based on polynomial functions like the well-known BPR function, we focus on routing games where an exponential function can specify the latency of road traffic. We first calculate a tight upper bound for the price of anarchy for this class of games and then compare this result with the tight upper bound of the PoA for routing games with the BPR latency function. The comparison shows that as long as the

traffic volume is lower than the road capacity, the tight upper bound of the PoA of the games with the exponential function is lower than the corresponding value with the BPR function. Finally, numerical results based on real-world traffic data demonstrate that the exponential function can approximate road latency as close as the BPR function with even tighter exponential parameters, which results in a relatively lower upper bound.

**Keywords:** Price of Anarchy, Congestion Game, Traffic Assignment, Multi-agent System

## 1 Introduction

Cities worldwide are confronted with numerous challenges in the context of sustainability and the livability of their environments. A study by the United Nations (UN) estimated that 68% of the world's population will live in cities by 2050 (Organization et al., 2019). Consequently, the increase in urban mobility places significant demand on urban traffic systems. The importance of sustainable management of the complex traffic system is amplified by the ecological footprint on the environment such as air quality, carbon dioxide emissions and overloaded infrastructure, as well as people's well-being related to traffic chaos, jams, noise and parking issues. These challenges pose practical resource allocation problems, among which traffic management is the highest priority.

Over the last decade, research on autonomous vehicles (AVs) has made revolutionary progress, bringing a promising solution to much safer, more convenient and more efficient transportation. Most significantly, advanced artificial intelligence (AI) allows self-driving cars to learn and adapt to complex road situations with millions of accumulated driving hours, much more than any experienced human driver could reach. The traffic assignment problem (Dafermos & Sparrow, 1969) is a typical resource allocation problem widely studied in transportation. This problem deals with how vehicles in a given road network choose their routes from their origins to their destinations. These vehicles, like human drivers, are assumed to make self-interested decisions to minimize the time they need to reach their destination. However, self-interested decision-making may be counter-productive since it may cause the total travel time to increase significantly compared to the globally optimal traffic assignment. The main motivation for our emphasis on autonomous driving is that vehicles have more powerful means of communication than humans to access more information about the road, which helps them make more rational decisions. However, we assume that vehicles decide which route to take when multiple routes are available for a specific origin-destination (OD) pair. This is a game-theoretical decision because if one route is shorter and all cars take that route, they only go slower due to congestion. The advent of self-driving vehicles and the gradual improvement of vehicle-to-everything (V2X) technologies make it possible to optimize vehicle routing on the road network globally.

The traffic assignment problem is usually defined formally using the congestion game model (Gibbons et al., 1992), in which the cost of each player is determined by

the resources it selects and the number of other players who make the same choice. Each road in the road network has an independent cost function that outputs the travel time of this road using the number of vehicles travelling on that road as input. In such a transportation system, the travel time of a vehicle depends on the chosen roads and the number of vehicles on the same road (Wang, Xiao, Xie, Frazzoli, & Rus, 2015).

In a road network, each vehicle is assumed as a non-cooperative agent (i.e. behaving selfishly) based on the assumption of a congestion game, aiming to find the best route with minimum cost (travel time) to reach its destination without considering the whole road network's performance. Traffic will reach a so-called user equilibrium (UE) if all vehicles decide selfishly, namely Wardrop's first principle (Wardrop, 1952a). At the user equilibrium state, no vehicle can achieve a shorter travel time by changing its route, implying that all vehicles with the same OD pair will have the same travel time. The selection of global optimization routes for a road network is called the system optimum (SO), known as Wardrop's second principle (Wardrop, 1952a), which reflects that the total travel time of all vehicles on the road network is minimized. This paper discusses the social aspects of autonomous driving, in particular, the behaviour of vehicles in different traffic conditions, including selfish behaviour and centralized control, from the game-theoretical point of view. Self-decision can be seen as decentralized control, whereas the pursuit of global optimization is centralized control.

It is well known that the self-interested decision-making of intelligent agents can cause degradation in the performance of the whole network (Akella, Seshan, Karp, Shenker, & Papadimitriou, 2002; Johari & Tsitsiklis, 2004). The Price of Anarchy (PoA), introduced by Koutsoupias and Papadimitriou (1999), is a concept in game theory that refers to the inefficiencies that arise in a system when individuals make decisions independently of each other without taking into account the overall impact of their actions. The PoA in transportation is the ratio between the optimal outcome that could be achieved if all individuals acted coordinated and efficiently and the actual outcome when individuals act independently. This concept is particularly relevant as it can lead to congestion and delays, which can be costly for individuals, businesses, and the economy as a whole. Understanding the PoA is crucial for transportation planners and policymakers seeking to optimize mobility and reduce the negative impacts of transportation on the environment and society. By identifying the sources of inefficiencies and developing strategies to mitigate them, transportation systems can be designed and managed more effectively and sustainably. In this study, PoA is adopted as an index to determine under what traffic situations individual decisions and centralized control are needed, respectively. The upper bound of PoA is investigated in this study for the worst-case over a large family of road networks with the same types of cost function (O'Hare, Connors, & Watling, 2016).

This paper aims to develop an expression of the tight upper bound of PoA for traffic assignment with exponential cost functions. We compare it with the expression of PoA when using the Bureau of Public Roads (BPR) function. This expression is related to the change in traffic demand. The final results show vehicles can make selfish decisions with low traffic volume. In contrast, global optimisation is taken when the traffic volume becomes higher. To achieve this, we first present a traffic assignment

model with related notation and properties about PoA. Then, we express changing traffic demand on the tight upper bound PoA with exponential cost functions in Table 1. After that, we simplify the complex expression to a more straightforward format. Next, we compare the differences between using the BPR and exponential functions to calculate PoA. In addition to the theoretical results, we use real-life traffic data from major Australian roads to explain the relevance of the exponential function and corroborate the theoretical results mentioned in the paper. The analysis results show that the exponential cost flow function matches the extracted data better than the previously studied cost flow functions.

The rest of this paper is organized as follows. Section 2 gives an overview of existing research related to our topic. In Section 3, we formally introduce the traffic assignment model and related notation. Section 4 gives a brief explanation and theoretical calculation to obtain the expression of the tight upper bound of the PoA for the road network with exponential cost functions. We present numerical examples and real-world data analysis to support the exponential cost function and theoretical results in Section 5. Finally, we summarize this paper and discuss future work in Section 6.

## 2 Related Work

Traffic assignment is a resource allocation problem, introduced by [Wardrop \(1952b\)](#), which describes how traffic demand is assigned to different routes when given the topology of the road network. It is one of the important research topics in the field of transportation. The congestion game, introduced by [Rosenthal \(1973\)](#), is a common-use model for formulating traffic assignments.

Many different cost flow functions have been proposed and used in practice. All these cost flow functions follow the basic principles of traffic flow theory, which state that speed decreases as the traffic flow or saturation rate increases. The saturation rate of a road is calculated as the relationship between traffic flow and capacity, where capacity is unknown and is a problem of estimation in transportation research ([Chen, Yang, Lo, & Tang, 1999](#); [Dheenadayalu, Wolshon, & Wilmot, 2004](#); [Morlok & Chang, 2004](#)). Before summarising the cost flow functions, we have to define some general concepts for the rest of this paper. The saturation ratio is  $x = \frac{f}{\phi}$ , where  $f$  is the traffic flow and  $\phi$  is the capacity of the road. The unit of road capacity and traffic flow is the number of vehicles per hour ([Division, 1964](#)).  $t_0 = \frac{l}{s}$  represents the free-flow travel time, where  $l$  is the length of the road and  $s$  the speed limit.

As an initial work, the cost flow function proposed by [Smock \(1962\)](#) was described as an exponential curve in the Detroit Area Transportation Study, and the value of the cost flow function shown in Equation (1) was estimated by averaging the intersection capacities at the ends.

$$t(x) = t_0 \cdot e^x \tag{1}$$

In 1965, [Soltman \(1966\)](#) proposed an exponential cost flow function, which is almost the same as the Smock function shown in Equation (1), in an integrated distribution-assignment model with application to the Pittsburgh Area Transportation Study.

$$t(x) = t_0 \cdot 2^x \quad (2)$$

where  $x \leq 2$ . In 1967, [Overgaard \(1967\)](#) proposed another function in the form below.

$$t(x) = t_0 \cdot ae^{x^b} \quad (3)$$

Among the well-developed cost flow functions, the BPR function is the most commonly used one ([Division, 1964](#)). Since its first publication in 1964, this model has been widely used among researchers in various traffic models due to its good balance between simplicity and effectiveness. In the BPR function shown in Equation (4), the ratio of travel time (or average travel speed) per unit of distance at practical capacity to free flow is defined by the parameter  $a$ . In contrast, the change of the average travel speed from free-flow to crowded conditions is determined by the parameter  $b$  ([Mtoi & Moses, 2014](#)).

$$t(x) = t_0 \cdot (1 + ax^b) \quad (4)$$

The default values of the parameters  $a$  and  $b$  are 0.15 and 4, respectively. However, these numbers do not reflect traffic conditions on all types of roads or in all traffic control methods ([Márquez, García, & Guarín, 2014](#)). In the actual applications, the parameters need to be adjusted accordingly. Therefore, a calibration process with extensive and accurate field data is needed. Despite its simplicity, unfortunately, this paradigm also comes with inherent drawbacks, mainly when the value of parameter  $b$  is high. Firstly, it suffers from overloaded links, meaning that the traffic flow is greater than the link capacity, appearing in the first few iterations of the traffic assignment when using the Method of Successive Averages (MSA) ([Liu, He, & He, 2009](#)). It slows the convergence by giving undue weight to overloaded links with a high value of  $b$ . Second, for connections far below capacity, the BPR function, especially under a high value of  $b$ , always produces free-flow travel time independent of the actual traffic flow.

Besides the BPR function, another widely used cost flow function is the Akcelik function ([Akcelik, 1978](#)) shown in Equation (5), a variant of the function proposed initially by [Taylor \(1997\)](#).

$$t(x) = t_0 + \frac{3600}{4}a[(x-1) + \sqrt{(x-1)^2 + \frac{8bx}{da}}] \quad (5)$$

where in the default values are  $a = 1$ ,  $b = 1$ ,  $c = 1$  and  $d = 1800$ . In addition to the aforementioned functions in literature, there are several other functions, such as the Vatzek function ([Jastrzebski, 2000](#)), the conical function ([Spiess, 1990](#)) and Mosher functions ([Mosher Jr, 1963](#)).

A great number of research on PoA from a game-theoretical point of view has been done ([Aland, Dumrauf, Gairing, Monien, & Schoppmann, 2011](#); [Christodoulou & Koutsoupias, 2005](#); [Feldman, Immorlica, Lucier, Roughgarden, & Syrgkanis, 2016](#)). The PoA in traffic assignment was first investigated by [Roughgarden and Tardos \(2002b\)](#). It is shown that the price of anarchy is precisely equal to  $\frac{4}{3}$  with linear cost functions. [Roughgarden \(2003\)](#) provides a theoretically tight upper bound of PoA

Description	Representative	Price of Anarchy
Linear	$ax + b$	$\frac{4}{3} \approx 1.333$
Quadratic	$ax^2 + bx + c$	$\frac{3\sqrt{3}}{3\sqrt{3}-2} \approx 1.626$
Cubic	$ax^3 + bx^2 + cx + d$	$\frac{4\sqrt[4]{4}}{4\sqrt[4]{4}-3} \approx 1.896$
Polynomial	$\sum_{i=0}^p a_i x^i$	$(1 - p(p+1)^{-\frac{p+1}{p}})^{-1}$
M/M/1 delay functions	$(u - x)^{-1}$	$\frac{1}{2}(1 + \sqrt{\frac{u_{min}}{u_{min} - R_{max}}})$
Exponential	$ae^{bx} + c$	$\frac{2b\hat{r}}{\log(b\hat{r}+1)}$

**Table 1:** The Upper Bound of PoA for Common Cost Functions (the last row (see Theorem 3) represents the proposed function in this paper).

to different cost functions, which are satisfy the continuous, non-negative, and non-decreasing, shown in Table 1. In previous studies, the main results of the upper bound of PoA depend on the characteristics of the cost function. For example, suppose a road network with polynomial cost functions, then the PoA is the maximum anarchy value of a road, which only depends on the exponent of the cost function on that road (Roughgarden, 2003). O’Hare et al. (2016) shows four mechanisms describing how PoA varies with traffic demand. More studies try to find PoA in terms of traffic demand. For example, a function that describes the relationship between traffic demand and PoA in the routing game is presented in (Cominetti, Dose, & Scarsini, 2021). In addition, there is some data-driven approach to estimate PoA (Zhang, Pourazarm, Cassandras, & Paschalidis, 2016, 2018).

### 3 Problem Formulation

In this section, we present a formal model to describe traffic assignment based on the definition of congestion game. This model is essentially the same as the one used in (Roughgarden, 2003) but rewritten in our notation. In short, we consider a network of roads with multiple origins and destinations. For each OD pair, a group of vehicles wants to travel from the origin to the destination. The number of vehicles for each OD pair is called the traffic demand.

We define a **road network** as a directed multigraph  $G = (V, P)$  with a set of positions  $V$  and a set of edges (roads)  $P$ <sup>1</sup>. In addition, parallel roads between two positions are allowed by the definition of a multigraph, but we do not allow self-loops.

An **origin-destination (OD)**  $(o, d) \in V \times V$  is a pair of locations (i.e., a pair of vertices of the graph  $G$ ) and  $OD = \{(o_i, d_i) : \forall i \in [1, k], o_i \in V, d_i \in V \setminus \{o_i\}\}$  denotes the set of all such origin-destinations in the road network  $G$ . For each origin-destination  $(o_i, d_i)$ ,  $\gamma$  is a sequence of roads called a **route**, which is a simple path (a path with no cycles) that links its origin  $o_i$  to its destination  $d_i$ . Let  $\Gamma_i$  denote all possible routes for  $(o_i, d_i)$  and  $\Gamma = \bigcup_{i \in [1, k]} \Gamma_i$  define all possible routes according to

<sup>1</sup>Here, we change the notation of the graph theory’s edge from  $E$  to  $P$ . The main reason is to avoid confusing the representation of the exponential function and the edge representation since the calculation related to the exponential function  $e$  is used extensively in the remainder of this paper.

the given topology of the road network  $G$ . We assume that for any  $i \in [1, k]$ ,  $\Gamma_i \neq \emptyset$ . **Traffic flow**  $f : \Gamma \rightarrow \mathbb{R}^+$  is a function that maps each route  $\gamma$  to a positive number that represents the traffic volume of that route, measured in the number of vehicles per hour. We use  $f_\gamma$  as a shorthand for  $f(\gamma)$  to simplify notation. For each OD  $(o_i, d_i)$ , we define the **traffic demand**  $r_i \in \mathbb{R}$  to be the total number of vehicles per hour that are travelling between  $o_i$  and  $d_i$ . We say that a flow  $f$  is **feasible** if and only if it satisfies  $\sum_{\gamma \in \Gamma_i} f(\gamma) = r_i$  for all  $i \in [1, k]$ , and we let  $F$  denote the set of all feasible flows. Furthermore, we define  $f_p = \sum_{\gamma \in \Gamma: p \in \gamma} f_\gamma$  as the traffic flow of the road  $p$  for a feasible flow  $f$ .

It is worth noting that all vehicles are assumed to have the same attributes, such as length and acceleration. Hence, homogeneous vehicle type is considered to focus on the time parameter, which is the only parameter affecting the travel cost function. Furthermore, we assume that vehicles do not have any special routing preference. For instance, if all vehicles are focused on reaching their destination in the shortest possible time, then only the time parameter is shown in the cost functions. Conversely, if trucks on the road seek only the minimum fuel consumption to reach their destination, SUVs demand the shortest path, and cars want the shortest travel time. This would make the cost function contain different units, fuel consumption, road length and time and use additional methods to transfer them to a unique unit.

Each road  $p \in P$  has a **cost function**  $l_p : \mathbb{R} \rightarrow \mathbb{R}$  that takes the **traffic flow**  $f_p$  of that road as its input and that outputs the travel time (in seconds) for a vehicle to drive along that road. The cost function should be non-negative, differentiable, and non-decreasing for obvious reasons; traffic leads to more road congestion and, thus, higher travel times. We use  $\mathcal{L}$  to denote a set of all possible cost functions, and, for some given road network  $G$ , we use  $L : P \rightarrow \mathcal{L}$  to denote the function that maps each road  $p$  to its corresponding cost function  $l_p$ . The travel time of a route  $\gamma \in \Gamma$  given a feasible traffic flow  $f \in F$  can be calculated as the sum of the travel times of the edges contained in the route, given by  $l_\gamma(f_\gamma) = \sum_{p \in \gamma} l_p(f_p)$ . The cost of a vehicle is the travel time of the route it selected. It should be noted that the travel time for each route is the average travel time of all vehicles that use the route. Furthermore, we define  $C(f) = \sum_{p \in P} l_p(f_p) f_p$  as the **social cost** incurred by the feasible flow  $f$ , which is the total travel time of all vehicles in the road network.

An **instance** of the traffic assignment problem is now defined as a tuple  $(G, \vec{r}, L)$ , where  $G$  and  $L$  are as above, and  $\vec{r} = (r_1, \dots, r_k)$  is a tuple containing the traffic demand  $r_i$  of each origin-destination  $(o_i, d_i)$ .

In transportation, *Wardrop's first principle*, also known as *user equilibrium (UE)*, has been accepted as a simple and sound principle to explain the distribution of traffic among alternative routes due to congestion. Traffic flows that adhere to this principle are referred to as equilibrium flows. Intuitively, each vehicle travels along the route with the minimum travel time. Otherwise, this vehicle would re-select other routes with lower travel time. The equilibrium flow is the result of purely self-interested decision-making. Formally, UE is defined as follows:

**Definition 1.** Given an instance  $(G, \vec{r}, L)$ , a feasible flow  $f \in F$  is a **user equilibrium (UE) flow** if and only if for any OD  $i \in [1, k]$  and any  $\gamma \in \Gamma_i$  with  $f_\gamma > 0$ , we have  $l_\gamma(f_\gamma) \leq l_{\gamma'}(f_{\gamma'})$  for any  $\gamma' \in \Gamma_i$ .

If all traffic is divided over the roads according to a UE flow, each vehicle cannot unilaterally change to a different route to obtain a shorter travel time. This means that when the traffic flow is at UE, for each origin-destination  $(o_i, d_i)$ , the travel time along each route between  $o_i$  and  $d_i$  that has a positive traffic flow is the same.

From existing work, it is known that any traffic assignment problem in the form of a congestion game is a potential game, and therefore there exists at least one pure strategy UE (Sandholm, 2010).

Furthermore, we note that if there exist two or more UE flows  $f$  and  $f'$ , then  $C(f) = C(f')$  for any instance  $(G, \vec{r}, L)$  (Roughgarden, 2005). Specifically, the UE flow of an instance is a traffic flow that minimizes the potential function, which can be calculated from a non-linear program (Sandholm, 2001).

A traffic flow is said to satisfy *Wardrop's second principle* (also known as *System Optimum (SO)*) if the average travel time of a feasible flow is at a minimum, achieving the global optimum of an instance  $(G, \vec{r}, L)$ . In other words, a SO flow is feasible with minimal social cost  $C(SO)$  among all feasible flows. Note that a System Optimum can only be reached if all vehicles choose their paths cooperatively to ensure the most efficient utilization of the system as a whole.

**Definition 2.** Given an instance  $(G, \vec{r}, L)$ , a feasible flow  $f^* \in F$  is a **system optimum (SO) flow** if and only if  $C(f^*) = \min_{f \in F} C(f)$ .

To explain how the minimal social cost can be calculated, the following definition is introduced.

**Definition 3.** For any cost function  $l$  its corresponding **marginal cost function**  $l^*$  is defined by  $l^*(x) := \frac{d}{dx}(x \cdot l(x))$ .

It is known from existing research (Beckmann, McGuire, & Winsten, 1956; Dafermos & Sparrow, 1969; Roughgarden & Tardos, 2002a), that for any instance  $(G, \vec{r}, L)$  a flow  $f \in F$  is an SO flow if and only if  $f$  is the UE flow for the corresponding instance  $(G, \vec{r}, L^*)$ , where  $L^* : P \rightarrow \mathcal{L}$  is a function that maps each road  $p$  to a cost function  $l_p^*$ , which is the marginal cost function corresponding to  $l_p$ . Therefore, we can get the SO flow of instance  $(G, \vec{r}, L)$  by finding the traffic flow with the minimum value of the potential function for instance  $(G, \vec{r}, L^*)$ .

The **price of anarchy (PoA)** is defined as the ratio between the social cost of the UE flow and the social cost of the SO flow for instance  $(G, \vec{r}, L)$ :

$$PoA(G, \vec{r}, L) := \frac{C(UE)}{C(SO)}$$

## 4 Price of Anarchy with Exponential Cost Functions

In this section, we derive an expression for an upper bound of the PoA in case all cost functions in the road network are exponential and show that this upper bound is tight. Furthermore, we present a more straightforward expression of the upper bound, which is not tight. It is worth mentioning that we only look at the theoretical results and proofs related to the exponential function in this section. The next section uses real-life traffic data to validate the proposed function further.

## 4.1 Exponential Cost Function

In this study, the travel cost on the road  $p \in P$  is expressed as an exponential function below:

$$l_p(f_p) = ae^{bf_p} + c \quad (6)$$

where  $f_p$  is the traffic flow of road  $p$  and  $a$ ,  $b$  and  $c$  are non-negative coefficients. These coefficients may differ for each road, so in the rest of the paper, if necessary, we will sometimes stress this by writing them as  $a_p$ ,  $b_p$ , and  $c_p$  instead. Furthermore, the values of  $a$ ,  $b$ , and  $c$  have ‘seconds’ as their unit (and since  $f_p$  was measured in the number of vehicles per hour, the product  $b \cdot f_p$  is unit-free).

The sum  $a + c$  is the free-flow travel time of road  $p$ , which depends on the speed limit and length of the road. We use  $\mathcal{L}_{exp}$  to denote the set of all possible cost functions of the form Eq.(6). Furthermore, we use  $(G, \vec{r}, L_{exp})$  to represent an instance with only exponential cost functions, so  $L_{exp} : P \rightarrow \mathcal{L}_{exp}$  is a function that maps each road to an exponential cost function, and we write  $l_p$  instead of  $L_{exp}(p)$  in the rest of this paper.

[Roughgarden \(2003\)](#) defined the notion of a *standard* function. A function  $l$  is standard if  $x \cdot l(x)$  is convex for  $x \geq 0$ . It is easy to see that any function of the form  $l(x) = ae^{bx} + c$  with non-negative coefficients is indeed standard. This fact will be useful to us later on. Furthermore, we note that an instance  $(G, \vec{r}, L_{exp})$  with only exponential cost functions has the special property of having a unique user equilibrium solution, as shown in the following theorem.

**Lemma 1.** *For any instance  $(G, \vec{r}, L_{exp})$ , there is a unique user equilibrium flow.*

*Proof.* From existing work ([Aashtiani & Magnanti, 1981](#); [Konishi, 2004](#); [Milchtaich, 2005](#)), it is known that a unique user equilibrium flow exists for any instance with monotonically increasing cost functions.  $\square$

## 4.2 Anarchy Value and Price of Anarchy

This subsection explores how to find the upper bound of the PoA for instances with exponential functions. We need to define the ‘anarchy value’ for each road, which is a cost ratio between the UE flow and SO flow of that road. The idea of anarchy value was proposed in [Roughgarden \(2003\)](#). The motivation to define the anarchy value is to find the worst-case ratio between the cost of UE flow and SO flow for a given set of cost functions.

It is worth mentioning that our definition of ‘anarchy value’ differs from the original one. The first main difference is that our definition depends on the traffic demand  $\vec{r}$  of the instance, while Roughgarden’s original definition took the supremum over all possible values of the traffic demand. The motivation for this difference is that otherwise, the upper bound of the PoA would go to infinity in the case of exponential cost functions. Secondly, our definition assumes that traffic is at user equilibrium. Formally, our definition of anarchy value is as follows.

**Definition 4.** *Let  $(G, \vec{r}, L_{exp})$  be an instance with exponential cost functions, and let  $f$  denote its user equilibrium flow. Then the **anarchy value**  $\phi_p(\vec{r})$  of a road  $p$  is defined as follows:*

$$\phi_p(\vec{r}) := [\lambda_p \mu_p + (1 - \lambda_p)]^{-1} \quad (7)$$

where  $\lambda_p \in [0, 1]$  is the solution of the equation  $l_p^*(\lambda_p f_p) = l_p(f_p)$ , and  $\mu_p$  is defined as  $\mu_p := \frac{l_p(\lambda_p f_p)}{l_p(f_p)} \in [0, 1]$ .

Note that the user equilibrium flow  $f^*$  depends on the traffic demand  $\vec{r}$ , so  $\lambda_p$  and  $\mu_p$  depend on  $\vec{r}$ , and therefore  $\phi_p$  also depends on  $\vec{r}$ . We need the following lemma to show that the anarchy value is well-defined.

**Lemma 2.** *For any function  $l$  of the form of Eq. (6) and for any positive value  $x \in \mathbb{R}^+$ , there is a unique value  $\lambda \in [0, 1]$  that solves the equation  $l^*(\lambda x) = l(x)$  (where  $l^*(\cdot)$  is the marginal cost function of  $l(\cdot)$ , see Def. 3)*

*Proof.* To prove this, we first note that

$$l^*(x) = ae^{bx} + abx \cdot e^{bx} + c \quad (8)$$

Secondly, we note that  $l$  and  $l^*$  monotonically increase on the domain  $x > 0$ . The idea is then to show that  $l^*(0) = l(0) \leq l(x) \leq l^*(x)$  is true for any positive  $x$ . It is easy to see that indeed we have  $l^*(0) = a + c = l(0)$ . Furthermore, since  $l$  is monotonically increasing, we have  $l(0) \leq l(x)$ . And finally, since  $a, b$  and  $x$  are all non-negative, we have:

$$l(x) = ae^{bx} + c \leq ae^{bx} + abxe^{bx} + c = l^*(x)$$

Since  $l$  and  $l^*$  are monotonically increasing and  $l^*(0) = l(0)$ , it is now easy to see that there exists a unique value  $x' \leq x$  such that  $l^*(x') = l(x)$ . Then, we can simply define  $\lambda := \frac{x'}{x} \in [0, 1]$ , so that indeed we have  $l^*(\lambda x) = l(x)$ .  $\square$

This lemma shows that  $\lambda_p$  and  $\mu_p$  of Def. 4 are well-defined. We now define  $\phi(L_{exp}) := \max_{p \in P} \phi_p(\vec{r})$  as the anarchy value of the instance  $(G, \vec{r}, L_{exp})$ . We can now show the relationship between the anarchy value and the PoA of an instance  $(G, \vec{r}, L_{exp})$  in the following Lemma.

**Lemma 3.** *For any instance  $(G, \vec{r}, L_{exp})$ , we have:*

$$PoA(G, \vec{r}, L_{exp}) \leq \phi(L_{exp})$$

*Proof.* Let  $f$  and  $f^*$  be UE flow and SO flow, respectively, for the given instance  $(G, \vec{r}, L_{exp})$ . From the Lemma 3.5 to Lemma 3.7 in Roughgarden (2003), it is easy to rewrite the social cost of SO in a form that is easier to relate to the social cost of UE as follows:

$$\begin{aligned} C(f^*) &\geq \sum_{p \in P} [l_p(\lambda_p f_p) \lambda_p f_p + (f_p^* - \lambda_p f_p) l_p(f_p)] \\ &\geq \sum_{p \in P} [\mu_p \lambda_p + (1 - \lambda_p)] l_p(f_p) f_p \end{aligned} \quad (9)$$

with  $\lambda_p$ ,  $\mu_p$  and  $f_p$  as in Def.4. Thus, we can rewrite this inequality as follows.

$$\begin{aligned} C(f^*) &\geq \sum_{p \in P} \frac{l_p(f_p)f_p}{[\mu_p\lambda_p + (1 - \lambda_p)]^{-1}} = \sum_{p \in P} \frac{l_p(f_p)f_p}{\phi_p(\vec{r})} \\ &\geq \frac{\sum_{p \in P} l_p(f_p)f_p}{\max_{p \in P} \phi_p(\vec{r})} = \frac{C(f)}{\phi(L_{exp})} \end{aligned} \quad (10)$$

Eq.(10) leads to

$$PoA(G, \vec{r}, L_{exp}) = \frac{C(f)}{C(f^*)} \leq \phi(L_{exp}) \quad (11)$$

□

From Lemma 3, we see that the PoA of any instance is always less than or equal to the maximum anarchy value over all roads in that instance.

### 4.3 The Lambert W Function

Before continuing with the rest of the paper, we here need to briefly discuss the Lambert  $W$  function (Corless, Gonnet, Hare, Jeffrey, & Knuth, 1996). For any positive real number  $x$ , the value  $W(x) \in \mathbb{R}$  is defined as the unique real number that satisfies:<sup>2</sup>

$$W(x)e^{W(x)} = x \quad (12)$$

The Lambert  $W$  function is monotonically increasing and satisfies the following well-known properties (Hoorfar & Hassani, 2007; Weisstein, 2002), which will be useful to us later on:

$$W(e) = 1 \quad (13)$$

$$\frac{d}{dx}W(x) = \frac{W(x)}{x \cdot (1 + W(x))} \quad (14)$$

For any  $x \geq e$ :

$$\log(x) - \log\log(x) \leq W(x) \leq \log(x) - \frac{1}{2}\log\log(x) \quad (15)$$

### 4.4 Upper Bound of the PoA

At this point, we have defined all the concepts required to calculate our upper bound of the PoA over the set of all instances  $(G, \vec{r}, L_{exp})$  with exponential cost functions. We present this upper bound below, in Theorem 1, which depends on two more lemmas.

**Lemma 4.** *For any instance  $(G, \vec{r}, L_{exp})$ , let  $f$  denote its user equilibrium flow. The anarchy value  $\phi_p(\vec{r})$  of any road  $p \in P$  with cost functions of the form  $l(x) = ae^{bx} + c$ , where  $a$ ,  $b$ , and  $c$  are non-negative coefficients, satisfies:*

---

<sup>2</sup>For real numbers  $x \in [-\frac{1}{e}, 0]$  this equation actually has two solutions, which are denoted as  $W_{-1}(x)$  and  $W_0(x)$  respectively, but in this paper, we are not interested in such values.

$$\phi_p(\vec{r}) \leq \frac{bx^*}{bx^* + 2 - W(e^{bx^*+1}) - \frac{1}{W(e^{bx^*+1})}} \quad (16)$$

where  $W(\cdot)$  is the Lambert  $W$  function and  $x^* = f_p$  is the UE flow of the road  $p$ .

*Proof.* Recall that the anarchy value is defined as  $\phi(\vec{r}) = [\lambda\mu + (1 - \lambda)]^{-1}$ , and to calculate  $\lambda$  we have to solve  $l^*(\lambda x^*) = l(x^*)$ , with  $l^*$  given by Eq.(8). That is, we have to solve:

$$ae^{\lambda bx^*} + a\lambda bx^* \cdot e^{\lambda bx^*} + c = ae^{bx^*} + c \quad (17)$$

Subtracting  $c$  from both sides and then dividing by  $a$  on both sides, we get:

$$\begin{aligned} e^{\lambda bx^*} + \lambda bx^* \cdot e^{\lambda bx^*} &= e^{bx^*} \\ (1 + \lambda bx^*) \cdot e^{\lambda bx^*} &= e^{bx^*} \\ (1 + \lambda bx^*) \cdot e^{\lambda bx^*+1} &= e^{bx^*+1} \end{aligned}$$

Next, if we replace  $(\lambda bx^* + 1)$  by  $\delta$ , then we get  $\delta e^\delta = e^{bx^*+1}$ , which can be solved using the Lambert  $W$  function. This gives us:  $\delta = W(e^{bx^*+1})$ . Now, if we substitute  $\lambda bx^* + 1$  back for  $\delta$ , and solve for  $\lambda$ , then we get the following:

$$\lambda = \frac{W(e^{bx^*+1}) - 1}{bx^*} \quad (18)$$

Next, recall that  $\mu$  was defined as  $\frac{l(\lambda x^*)}{l(x^*)}$ , so we have:

$$\mu = \frac{ae^{\lambda bx^*} + c}{ae^{bx^*} + c}$$

We note that  $\mu$  therefore satisfies:

$$\mu \geq \frac{ae^{\lambda bx^*}}{ae^{bx^*}} = e^{(\lambda-1)bx^*} \quad (19)$$

Plugging these expressions (18) and (19) for  $\lambda$  and  $\mu$  back into  $[\lambda\mu + (1 - \lambda)]^{-1}$ , we obtain:

$$\begin{aligned} \phi(\vec{r}) &= [\lambda\mu + (1 - \lambda)]^{-1} \\ &\leq \left[ \frac{W(e^{bx^*+1}) - 1}{bx^*} \cdot e^{(W(e^{bx^*+1})-1)bx^*} + 1 - \frac{W(e^{bx^*+1}) - 1}{bx^*} \right]^{-1} \\ &= \left[ \frac{W(e^{bx^*+1}) - 1}{bx^*} \cdot e^{(W(e^{bx^*+1})-1)bx^*} + \frac{bx^*}{bx^*} - \frac{W(e^{bx^*+1}) - 1}{bx^*} \right]^{-1} \\ &= \frac{bx^*}{(W(e^{bx^*+1}) - 1) \cdot e^{(W(e^{bx^*+1})-1)bx^*} + bx^* - (W(e^{bx^*+1}) - 1)} \end{aligned}$$

We see from Eq.(12) that for any  $x > 0$  we have  $e^{W(x)} = \frac{x}{W(x)}$ , so we have

$$e^{W(e^{bx^*+1})-1-bx^*} = \frac{e^{bx^*+1}}{W(e^{bx^*+1})} \cdot e^{-1-bx^*} = \frac{1}{W(e^{bx^*+1})}$$

From this, we get the following:

$$\begin{aligned} \phi(\vec{r}) &\leq \frac{bx}{(W(e^{bx+1}) - 1) \cdot \frac{1}{W(e^{bx+1})} + bx - (W(e^{bx+1}) - 1)} \\ &= \frac{bx}{bx + 2 - W(e^{bx+1}) - \frac{1}{W(e^{bx+1})}} \end{aligned} \quad (20)$$

□

The following two lemmas give us a better idea of how the expression at the end of Eq.(20) behaves.

**Lemma 5.** *The following equation holds:  $\lim_{x \rightarrow 0} \frac{x}{x+2-W(e^{x+1})-\frac{1}{W(e^{x+1})}} = 1$*

*Proof.* Instead of proving this directly, we will prove the ‘reversed’ equation, which is equivalent:

$$\lim_{x \rightarrow 0} \frac{x + 2 - W(e^{x+1}) - \frac{1}{W(e^{x+1})}}{x} = 1 \quad (21)$$

This means we need to prove the following:

$$\lim_{x \rightarrow 0} \frac{2 - W(e^{x+1}) - \frac{1}{W(e^{x+1})}}{x} = 0 \quad (22)$$

Now, note that since  $\lim_{x \rightarrow 0} W(e^{x+1}) = 1$ , we can multiply this by  $W(e^{x+1})$ . So, equivalently we can prove the following:

$$\lim_{x \rightarrow 0} \frac{2 \cdot W(e^{x+1}) - W(e^{x+1})^2 - 1}{x} = 0 \quad (23)$$

Note that, in this equation, the limit of both the numerator and the denominator is 0, so we can calculate this limit using L’Hopital’s rule. Indeed, using Eq.(14) we get:

$$\begin{aligned} \lim_{x \rightarrow 0} \frac{2W(e^{x+1}) - W(e^{x+1})^2 - 1}{x} &= \lim_{x \rightarrow 0} \frac{\frac{d}{dx}(2W(e^{x+1}) - W(e^{x+1})^2 - 1)}{\frac{d}{dx}x} \\ &= \lim_{x \rightarrow 0} \frac{\frac{d}{dx}(2W(e^{x+1}) - W(e^{x+1})^2 - 1)}{1} \\ &= \lim_{x \rightarrow 0} \frac{d}{dx}(2W(e^{x+1}) - W(e^{x+1})^2 - 1) \\ &= \lim_{x \rightarrow 0} \left( \frac{2W(e^{x+1})}{W(e^{x+1}) + 1} - \frac{2W(e^{x+1})^2}{W(e^{x+1}) + 1} \right) \end{aligned} \quad (24)$$

Then, applying Eq.(13) we get:

$$\begin{aligned}
\lim_{x \rightarrow 0} \frac{2W(e^{x+1}) - W(e^{x+1})^2 - 1}{x} &= \lim_{x \rightarrow 0} \left( \frac{2W(e^{x+1})}{W(e^{x+1}) + 1} - \frac{2W(e^{x+1})^2}{W(e^{x+1}) + 1} \right) \\
&= \lim_{x \rightarrow 0} \left( \frac{2W(e)}{W(e) + 1} - \frac{2W(e)^2}{W(e) + 1} \right) \\
&= \lim_{x \rightarrow 0} \left( \frac{2}{2} - \frac{2}{2} \right) \\
&= 0
\end{aligned} \tag{25}$$

□

**Lemma 6.** *The expression  $\frac{x}{x+2-W(e^{x+1})-\frac{1}{W(e^{x+1})}}$  is monotonically increasing for  $x > 0$ .*

*Proof.* To prove this, we calculate its derivative and show that it is non-negative for any positive  $x$ .

$$\begin{aligned}
\frac{d}{dx} \frac{x}{x+2-W(e^{x+1})-\frac{1}{W(e^{x+1})}} &= \frac{(x+1-W(e^{x+1})) \cdot (W(e^{x+1})-1) \cdot W(e^{x+1})}{(W(e^{x+1})^2 - (x+2) \cdot W(e^{x+1}) + 1)^2} \\
&= \frac{(x+1-W(e^{x+1})) \cdot (W(e^{x+1})-1) \cdot W(e^{x+1})}{(W(e^{x+1})^2 - (x+2) \cdot W(e^{x+1}) + 1)^2}
\end{aligned} \tag{26}$$

It is easy to see that the denominator is non-negative. For the numerator, we divide into three parts:  $x+1-W(e^{x+1})$ ,  $W(e^{x+1})-1$ , and  $W(e^{x+1})$ . Since the Lambert  $W$  function is monotonically increasing and  $W(e) = 1$ , we can easily see that  $W(e^{x+1})-1$  and  $W(e^{x+1})$  are both non-negative. For the remaining expression, we note that it is 0 when  $x = 0$ , and that (by Eq.(14)) we have

$$\frac{d}{dx}(x+1-W(e^{x+1})) = \frac{1}{W(e^{x+1})+1} \geq 0$$

From this, it follows that  $x+1-W(e^{x+1})$  is also non-negative for any positive value of  $x$ . □

The following theorem gives us an upper bound for the PoA of any instance  $(G, \vec{r}, L_{exp})$  with exponential cost functions. We first need to introduce the following notation:  $\hat{r} := \sum_{i \in [1, k]} r_i$  and  $\hat{b} := \max_{p \in P} b_p$

**Theorem 1.** *For any instance  $(G, \vec{r}, L_{exp})$  with exponential cost functions, the price of anarchy satisfies the following.*

$$PoA(G, \vec{r}, L_{exp}) \leq \frac{\hat{b}\hat{r}}{\hat{b}\hat{r} + 2 - W(e^{\hat{b}\hat{r}+1}) - \frac{1}{W(e^{\hat{b}\hat{r}+1})}} \tag{27}$$

*Proof.* We know from Lemma 3 that:

$$PoA(G, \vec{r}, L_{exp}) \leq \phi(L_{exp}) = \max_{p \in P} \phi_p(\vec{r})$$

Then, we know from Lemma 4 that  $\phi_p(\vec{r})$  can be replaced by the right-hand side of Eq.(16). Furthermore, thanks to Lemma 6 and the fact that  $f_p^* \leq \hat{r}$  we can replace  $f_p^*$  by  $\hat{r}$ . Similarly, again thanks to Lemma 6 and the fact that  $b_p \leq \hat{b}$  we can remove the maximization over  $p \in P$  and instead simply replace  $b_p$  by  $\hat{b}$ . Hence, we obtain Eq.(27).  $\square$

## 4.5 Tightness of the Upper Bound

The following Theorem shows that the expression we presented in Theorem 1 is, in fact, a *tight* upper bound for the set of all instances with exponential functions.

**Theorem 2.** *For any positive numbers  $\hat{b}$  and  $\hat{r}$ , there exists an instance  $(G, \vec{r}, L_{exp})$  with exponential cost functions, for which  $PoA(G, \vec{r}, L_{exp})$  is exactly equal to*

$$\frac{\hat{b}\hat{r}}{\hat{b}\hat{r}+2-W(e^{\hat{b}\hat{r}+1})-\frac{1}{W(e^{\hat{b}\hat{r}+1})}}.$$

*Proof.* We prove this theorem using a simple road network, which is an adaptation of a road network known as *Pigou's example* (Pigou & Aslanbeigui, 2017), shown in Fig.1. Network (a) in this figure is the network for which we will calculate the PoA. We can choose any arbitrary number  $r$  as the traffic demand for this network (i.e.  $\vec{r} = (r)$ ). Network (b) is the same network but with the cost functions replaced by their corresponding marginal cost functions. To calculate the PoA of the network (a), we first need to calculate its UE flow. As explained above, to do this, we need to set the latency  $l_{p'}$  of the lower road  $p'$  equal to the latency  $l_p$  of the upper road  $p$ . That is, we need to solve equation  $e^{br} = e^{bx}$ , which leads to  $x = f_{p'} = r$ . This means that all traffic is choosing the lower road  $p'$ . The total cost  $C(UE)$  is then given by:

$$C(UE) = f_{p'} \cdot l_{p'}(f_{p'}) = r \cdot l_{p'}(r) = r \cdot e^{br}$$

Next, we need to calculate the SO flow for network (a), which is equal to the UE flow of network (b). So, we need to set the latency of the two roads in network (b) equal. That is, we need to solve:  $e^{br} = e^{bx}(bx + 1)$ , for which the solution is given by:  $x = \frac{W(e^{br+1})-1}{b}$ . This means that in the SO flow, the total number of vehicles choosing the lower road is given by  $f_{p'} = \frac{W(e^{br+1})-1}{b}$  and the total number of vehicles choosing the upper road is  $f_p = r - \frac{W(e^{br+1})-1}{b}$ . The total cost of  $C(SO)$  for all vehicles is then given by:

$$\begin{aligned} C(SO) &= f_p \cdot l_p(f_p) + f_{p'} \cdot l_{p'}(f_{p'}) \\ &= \frac{W(e^{br+1})-1}{b} \cdot e^{W(e^{br+1})-1} + \left(r - \frac{W(e^{br+1})-1}{b}\right) \cdot e^{br} \end{aligned}$$

where  $p$  is the upper road of the network and  $p'$  is the lower road. Combining these two results we get:

$$\begin{aligned}
PoA &= \frac{r \cdot e^{br}}{\frac{W(e^{br+1})-1}{b} \cdot e^{W(e^{br+1})-1} + (r - \frac{W(e^{br+1})-1}{b}) \cdot e^{br}} \\
&= \frac{br \cdot e^{br}}{(W(e^{br+1}) - 1) \cdot e^{W(e^{br+1})-1} + (br - W(e^{br+1}) + 1) \cdot e^{br}}
\end{aligned}$$

From Eq.(12) we see that for any  $x > 0$  we have  $e^{W(x)} = \frac{x}{W(x)}$ , so we have

$$e^{W(e^{br+1})-1} = \frac{e^{br+1}}{e \cdot W(e^{br+1})} = \frac{e^{br}}{W(e^{br+1})}$$

Using this, we get:

$$\begin{aligned}
PoA &= \frac{br \cdot e^{br}}{(W(e^{br+1}) - 1) \cdot \frac{e^{br}}{W(e^{br+1})} + (br - W(e^{br+1}) + 1) \cdot e^{br}} \\
&= \frac{br}{(W(e^{br+1}) - 1) \cdot \frac{1}{W(e^{br+1})} + (br - W(e^{br+1}) + 1)} \\
&= \frac{br}{br + 2 - W(e^{br+1}) - \frac{1}{W(e^{br+1})}}
\end{aligned}$$

Finally, since this example only had one value  $b_p$  and one value  $r_i$ , we have  $\hat{b} = b$  and  $\hat{r} = r$ , so we have indeed wave obtained the expression mentioned in the theorem.  $\square$

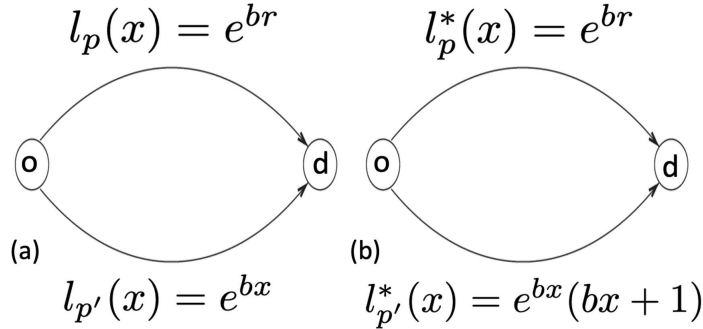


**Fig. 1:** A Variant of Pigou's example

## 4.6 Alternative Upper Bound

The tight upper bound we presented in Theorem 1 has a rather complex expression. Therefore, we will now derive two simpler expressions that form a lower- and upper-

bound for this expression. It shows that the original expression grows less than linearly as a function of  $\hat{b}$  and  $\hat{r}$ .

**Lemma 7.** *For any non-negative  $x$ , we have*

$$\frac{x}{\log(x+1)} \leq \frac{x}{x+2-W(e^{x+1})-\frac{1}{W(e^{x+1})}} \leq \frac{2x}{\log(x+1)}$$

*Proof.* Since  $x$  is non-negative we have  $e^{x+1} \geq e$ , so we can substitute  $e^{x+1}$  for  $x$  in Eq.(15) and obtain:

$$x+1-\log(x+1) \leq W(e^{x+1}) \leq x+1-\frac{1}{2}\log(x+1)$$

From this we get:

$$\begin{aligned} \frac{x}{x+2-W(e^{x+1})-\frac{1}{W(e^{x+1})}} &\leq \frac{x}{\frac{1}{2}\log(x+1)+1-\frac{1}{x+1-\log(x+1)}} \\ &\leq \frac{2x}{\log(x+1)} \end{aligned} \quad (28)$$

where we used the fact that  $\frac{1}{x+1-\log(x+1)} < 1$ , and we get:

$$\begin{aligned} \frac{x}{x+2-W(e^{x+1})-\frac{1}{W(e^{x+1})}} &\geq \frac{x}{\log(x+1)+1-\frac{1}{x+1-\frac{1}{2}\log(x+1)}} \\ &\geq \frac{x}{\log(x+1)} \end{aligned} \quad (29)$$

where we used the fact that  $\frac{1}{x+1-\frac{1}{2}\log(x+1)} < 1$ .  $\square$

It is worth mentioning that the function in Eq.(28) and Eq.(29) is monotonically increasing for non-negative  $x$ . From Lemma 7, we can easily obtain the following theorem.

**Theorem 3.** *For any instance  $(G, \vec{r}, L_{exp})$  with exponential cost functions, its price of anarchy satisfies:*

$$PoA(G, \vec{r}, L_{exp}) \leq \frac{2\hat{b}\hat{r}}{\log(\hat{b}\hat{r}+1)}$$

*Proof.* This is simply the combination of Theorem 1 and Lemma 7.  $\square$

## 5 Data and Numerical Results

To further validate the proposed function, real-world data is adopted for numerical experiments in this section. It is worth mentioning that the basic assumption in this chapter is to consider an administrative region as a road segment of the road network. First, we introduce the Australian traffic database involved in this paper and the basis for data selection. Next, we review the parameters related to data analysis. Then the accuracy of the exponential function, the BPR function and the Akcelik function are fitted and analyzed separately for different periods. Last, we compare the expression of tight upper bound PoA between the BPR function and the exponential function.

## 5.1 Data Description

In this study, Insight, a traffic database provided by Intelmatic, is employed, which covers more than 40,000 km of roads in New South Wales (NSW) and Victoria (VIC) in Australia with traffic flow data and speed data from 2019 to date. In terms of data frequency, it records data every 15 minutes. Regarding the coverage scope, it ranges from individual link-based data (microscopic level) to Local Government Area (LGA) (macroscopic level). The data used in this paper is within NSW, covering 39 LGAs, 1058 suburbs and nearly 5000 covered roads in NSW, which have a total length of nearly 19,500 km. Located on the southeast coast of Australia, the Greater Sydney region is the capital of the Australian state of New South Wales. It is the largest and most populous city in Australia. The Sydney metropolitan area has an area of approximately  $1687 \text{ km}^2$  and a population of approximately 5.73 million in 2019. The data between January 2019 and March 2022 are used in time intervals of years, months, weeks, days and even 15 minutes. We filter the data following the criteria below to derive more accurate traffic and travel time correlation functions.

- To best fit the cost function, the sampling region must include as many types of roads as possible, including viaducts, freeways, and urban roads.
- The absence of overlapping areas in the sampling area ensures the regional road network's independence and distinctive topological features.
- The sampling region must feature a variety of land uses, including commercialized areas, high-density office sectors, residential areas with a mix of high and low densities, and a well-connected road system.
- Fitting function data must be sampled over a wide time interval to prevent the impact of crises on traffic data, such as automobile accidents, special holidays, and lengthy traffic control.
- The selected area needs to have prevailing traffic conditions.

After filtering, three LGAs (i.e., Sydney, North Sydney and Parramatta) belonging to the Greater Sydney Area with high traffic flow and population density are selected for analysis considering that these areas can cover a wide range of traffic conditions. In addition to the three LGAs, we also select a suburb from each with similar characteristics as described above.

### 5.1.1 Sydney

The City of Sydney is a local government district in the Sydney Metropolitan Area of NSW, comprising the Sydney Central Business District (CBD) and 31 adjacent suburbs. The City of Sydney has a population of approximately 170,000 and a land area of 6.19 square kilometres. The area is a major financial, commercial and tourist centre with a large transient population and an extensive road network. As a result, the traffic situation is complex, consisting of many urban roads, underground tunnels and highways connecting neighbouring areas. The data we use covers 461 roads in Sydney's local government area, which are a total of 433 km long.

### 5.1.2 North Sydney

North Sydney is a local government area on the Lower North Shore of Sydney. It has a population of 67,658 and covers an area of approximately 10.9 square kilometres. The area has many high-density commercial areas, complex urban roads, toll roads and free expressways that connect the rest of Sydney. The North Sydney LGA data covers 156 roads with 166 km total length and 14 suburbs under its jurisdiction.

### 5.1.3 Parramatta

The City of Parramatta spans 84 square kilometres. According to the 2016 census, Parramatta has a population of 226,149 and contains 38 suburbs within its jurisdiction. This busy area covers several highways that run through the Sydney area, as well as complex urban roads. Parramatta LGA's database includes 222 roads with a total length of 470 km.

### 5.1.4 Suburb Selection

For the selection of suburban data, we use the traffic data from the central city of the three LGAs mentioned above as base data for comparison. The study area includes a central business district with multiple high-rise buildings, a mixed commercial and residential high-density region, a relatively low-density residential neighbourhood, and a substantial urban highway network. Even under identical traffic conditions, the transportation networks in the selected areas have different traffic capacities and road conditions due to differences in topographic characteristics.

## 5.2 Data Structure

The data in the Insight database was collected from numerous sources and validated to provide road and traffic statistics. Real-time detectors (GPS hardware) from commercial and private fleets of road vehicles and millions of nodal sensors at highways and intersections are used to collect real-time traffic flow and speed. Real-time data on road conditions from emergency services and road management provide the context for further calibration of the data sources. Cross-validation of 24/7 field control groups and machine learning algorithms ensures the validity of the data. We use vehicle data from the Insight database in multiple NSW LGAs, and suburbs to compare the proposed exponential function to other existing cost flow functions. The LGA and suburban data from January 1, 2019, to February 28, 2022, consisting of speed data and traffic flow data. The speed data contains the average speed, average delay time, average travel time, road ID, area ID, the total length of the entire road, and the average speed limit for the peak and non-peak periods within the area during the time interval. The flow data contains the total traffic flow in an area, road ID, area ID, and total length of roads throughout the area during peak and off-peak periods within the time interval.

The data is obtained by integrating the data of all road sections in the jurisdiction every 15 minute. The relevant data is divided into peak and off-peak periods by day. The peak period is 8 hours in total, including 7 am to 10 am and 3 pm to 6 pm from

Monday to Friday, while the off-peak period is 16 hours (excluding the peak period) plus 24 hours per day on weekends (Saturday and Sunday). It is worth noting that in the data analysis section, data on public holidays is merged into the off-peak period. Section 3 averages the data and uses the traffic flow per hour as the base unit. The peak period data is averaged over all 8 hours, the weekday off-peak data is divided by 16 to obtain the hourly average, and the non-working day and holiday data are divided by 24 hours to obtain the average. In addition, the traffic flow and road capacity mentioned in this paper are macro parameters within a region. They are obtained by summing the capacity or flow of all regional road segments.

### 5.3 Evaluation Criteria

For comparison, we use the data set on the commonly used BPR and Akcelik functions. The aim is to identify and analyze the advantages and disadvantages of each function. To compare with a unified standard, we simplify the three functions in the following way.

$$l(x) = ax^b + c \quad (BPR) \quad (30)$$

$$l(x) = c + \frac{3600}{4}a[(x-1) + \sqrt{(x-1)^2 + \frac{8b \cdot x}{\Phi \cdot a}}] \quad (Akcelik) \quad (31)$$

where  $\Phi$  is the capacity of the road, and the coefficient of determination, abbreviated  $R^2$ , is the proportion of variation in the dependent variable that the independent variable can predict in statistics. It is a statistical criterion used to predict future outcomes or to evaluate hypotheses based on other data. Based on the fraction of the total variation of effects explained by the model, it measures how well the observed results are represented by the model (Carpenter, 1960; Glantz & Slinker, 2001).

The function fit analysis uses traditional  $R^2$  and root-mean-square error (RMSE). We use the R-squares of different equations in the same region to illustrate how well the function fits.

$$R^2 = 1 - \frac{\sum_{i=0}^N (y_i - \hat{y}_i)^2}{\sum_{i=0}^N (y_i - \bar{y}_i)^2} \quad (32)$$

where  $N$  is the number of samples,  $y_i$  is a dependent variable,  $\hat{y}_i$  is the output of the regression model, both indexed by data set  $i$  and  $\bar{y}_i$  is the mean of the dependent variable.  $R^2$  is always less than or equal to 1; the larger it is, the more the variance of the dependent variable is explained by the regression model.

The RMSE is a commonly used metric for comparing predicted and observed values (sample or population values) by a model or estimator (Li, Zhao, Zhou, Palicot, & Zhang, 2014; Xie, Zhang, & Ye, 2007). It is also one of the parameters commonly used in the transportation field for the degree of fit between functions and data. The square root of the second sample moment of the discrepancies between anticipated and observed values, or the quadratic mean of these differences, is represented by the RMSE. The RMSE combines the magnitudes of prediction mistakes for different data points into a single measure of predictive capacity. To compare the forecasting mistakes of other models, the RMSE measures accuracy.

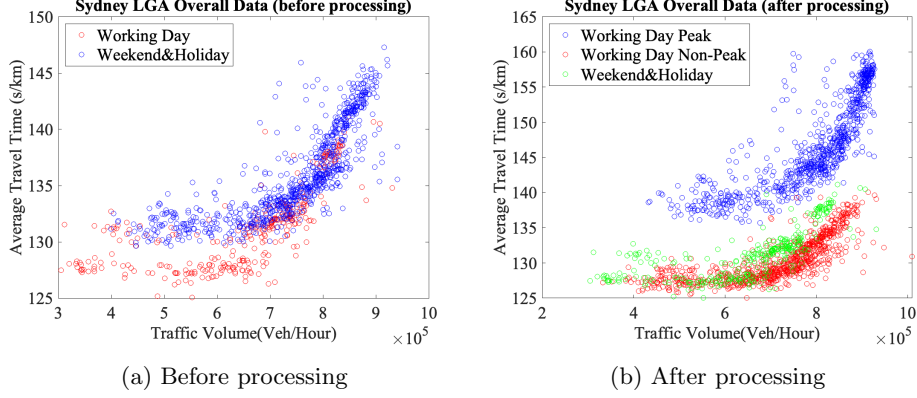


**Fig. 2:** Daily Data in Sydney

$$RMSE = \sqrt{\frac{\sum_{i=0}^N (y_i - \hat{y}_i)^2}{N}} \quad (33)$$

where  $N$  is the number of samples,  $y_i$  is a dependent variable,  $\hat{y}_i$  is the output of the regression model. We use  $R^2$  and RMSE as reference quantities for the degree of fit of the data to the function. The closer the  $R^2$  is to 1, the better the function fits the data; conversely, the higher the RMSE, the worse the function fits the data.

## 5.4 Curve Fitting Results

This section analyses the differences between the different cost flow functions in different regions. Firstly, we perform statistical analysis and function fitting on peak-hour and nonpeak-hour data at the LGA level. Then we narrow down the regions from LGAs to suburbs. The results of our preliminary analysis indicate a clear data stratification based on the data set. The phenomenon can be described as a clear regionalization of the data point set. We cut the Y-axis data within the same X-axis interval into multiple mutually independent fetches. We used data from Sydney as an example to explain data stratification.

The average velocity of different time intervals is used as raw data for processing. The average travel time required to complete one kilometre in different traffic flows is obtained using the equation relating speed to road length. Fig.2a shows the daily data in Sydney LGA from January 1, 2019, to February 28, 2022. The X-axis represents the traffic flow per hour, while the Y-axis represents the average time (in seconds) it takes a car to drive one kilometre. The upper stratification (blue points) is composed of weekdays (Monday-Friday), while the lower one (red points) consists of weekends (Saturday-Sunday) and public holidays. Since the data are divided into multiple data point sets, the data can be split into multiple independent areas. The daily data are unsuitable for data fitting by a single cost flow function. In this case, we split the data into peak and off-peak periods. Fig.2b shows the set of data points after splitting the data. Each point in the figure shows the traffic flow (Veh/hour) and the travel time

(s / km) during the peak and off-peak periods. As can be seen in the figure, there are three clusters. Further analysis of the data reveals that the top group (blue points) is the set of data points during peak hours on weekdays; the bottom group (red points) is the set of data points during off-peak hours on weekdays, and the middle group (green points) is the set of data points on weekends or holidays. The data in Fig. 2 indicate that the travel time varies between partitions for the same traffic. During that period, the volume of traffic within a specific period will be significantly higher than at other times. Although the average flows are similar, the distribution of traffic in specific hourly intervals is different. We can use an easy-to-understand example to explain that the distribution of traffic during peak hours is more like a normal distribution, whereas the distribution of traffic during off-peak hours and holidays is like a uniform distribution. Although the average values of traffic flows are the same, the average travel times are different because the relationship between traffic flows and travel times is non-linear from observations. Furthermore, traffic control schemes are inconsistent over time, resulting in variation. Additionally, some temporary traffic controls are implemented during off-peak hours. Therefore, we fit the Sydney LGA traffic data into three cases, as mentioned above.

In the following of this section, we first fit the data for the three LGA peak hours to three different cost flow functions. Second, we fit the data for the Sydney LGA as an example to distinguish between working off-peak hours and holidays&weekend by comparing the exponential function, the BPR function, and the Akcelik function. Next, we reduce the area size from LGA to suburbs and use the same approach to fit the data and compare the related functions. Finally, we summarize the results of the data analysis. It is worth mentioning that the fitting results covered in this section are the average travel time required to complete one kilometre in the area under different traffic flow conditions.

#### 5.4.1 Working Day Peak Hours

First, we fit the functions using the working day peak hour data for the three regions mentioned in Section 2. Peak hours on working days are defined as between *7am* and *10am*, and *3pm* and *6pm* from Monday to Friday. Fig.3 synthetically shows how the three cost flow functions fit the peak hours in the three LGAs. Figs.3(a) shows the geographic information of the three LGAs. Fig.3(b)-(d) show the road data fitted by different functions in the Sydney, Parramatta, and North Sydney LGAs, respectively. It can be observed that the fit of the exponential function is very similar to the BPR function. On the contrary, the second half of the Akcelik function differs significantly from the remaining two functions regarding areas not covered by the data. However, the fits of the three functions to the data intervals are similar, differing in the gradient after exceeding the area capacity. One of the exponential functions has a bigger gradient change than the BPR function. Therefore, it can be seen that the exponential function is the best fit of the three functions in the fit of the data in the peak period.

Table 2 shows the capacity and function factors of the different LGAs. It can be seen that different LGAs have different maximum capacities. The value of  $c$  in the table reflects a surprising consistency between different equations in the same region. This value represents the average free-flow travel time for all roads in the region, which

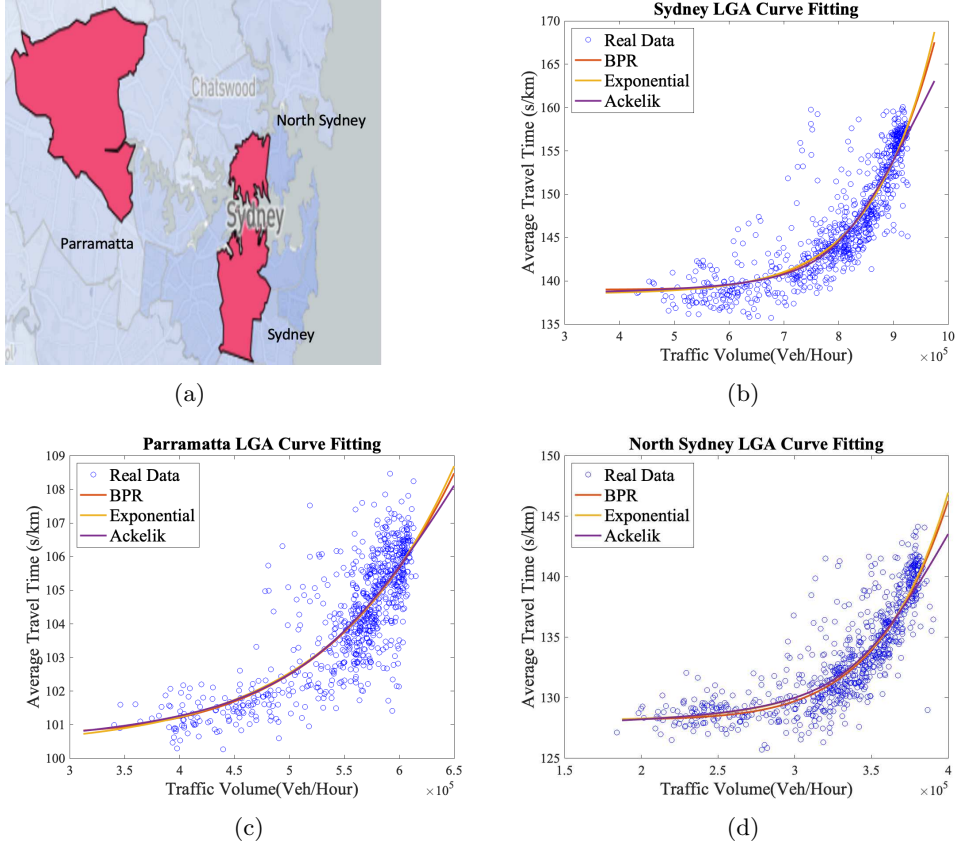


**Fig. 3: LGA Peak Hour Results**

**Table 2: Results in the LGA Peak Hours**

Region	Model	Capacity (V/H)	a	b	c	$R^2$	RMSE
Sydney	BPR	900000	6.494	8.12	139	0.7847	2.971
	Akcelik	900000	0.06193	60.88	138.4	0.7813	2.994
	Exponential	900000	0.004602	7.325	138.5	0.7856	2.965
Parramatta	BPR	580000	3.463	5.598	100.7	0.6434	1.062
	Akcelik	580000	0.01983	535.5	100.3	0.6438	1.059
	Exponential	580000	0.02734	4.956	100.3	0.6443	1.058
North Sydney	BPR	280000	5.735	8.592	128.2	0.7562	2.088
	Akcelik	280000	0.051	371	127.6	0.756	2.089
	Exponential	280000	0.001908	8.049	128.1	0.7568	2.08

implies the time it takes a vehicle to travel on a road at the maximum allowed speed. It can be concluded that the exponential function has the best  $R^2$ , and the value of RMSE is inversely proportional to the growth of  $R^2$ . Since the different distribution

of data concentrations in each region can lead to an irregular variation of  $R^2$ , we only compare the fit between different functions in the same region rather than performing a uniform analysis of all regions.

We use the parameters in Table 2 to analyze the fit in different traffic flows. Traffic flows are divided into three cases: low flow ( $0 \leq x < 0.5$ ), high flow ( $0.5 \leq x < 1$ ), and overflow ( $x > 1$ ). Table 3 shows the results obtained by partitioning and refining the data using the fit functions of the data to the BPR and exponential functions. From the results, it can be seen that the fit results of the exponential function are always higher than the results of the BPR function, indicating that the exponential function is better matched to the real data under different flow conditions.

**Table 3:** Curve Fitting Results

Region	Functions	Low flow	High flow	Overflow	Overall
Sydney	BPR	0.2926	0.241	0.5151	0.7847
	Exponential	0.3053	0.2438	0.5161	0.7856
Parramatta	BPR	0.6121	0.4822	0.5846	0.6434
	Exponential	0.6141	0.4838	0.5850	0.6443
North Sydney	BPR	0.2884	0.1755	0.6398	0.7562
	Exponential	0.2979	0.1768	0.6418	0.7568

#### 5.4.2 Working Day Off-peak Hours

Fig.4 shows all the data during the working day off-peak period and holidays in the Sydney LGA, from which it can be seen that the data are divided into several different groups due to different road conditions on working days and weekends&holidays. It is worth mentioning that since there are still different categories in the off-peak data for public holidays and weekends and workdays, we analyze the data for off-peak days on weekdays and weekends&holidays separately.

Fig.5(a) shows the results of the road data and the adjustment of the function for off-peak weekday hours, and Fig.5(b) shows the results of the road data and the adjustment of the function for holidays and weekends. Compared to the peak period, the traffic flow variation interval is relatively small during the weekday off-peak period, leading to the conclusion that traffic flow is also relatively stable during the weekday off-peak period. However, data for weekends and holidays show a distribution similar to that of the peak period, indicating that traffic flow is relatively more variable at different times.

Table 4 shows the coefficients and parameters fitted for each function in different cases. In terms of parameters and fits, they are essentially the same as for the LGA zone data, except that the Akcelik function fits slightly better than the other two functions on weekends, which is caused by the small sample size of the data and the relative dispersion of the data in the intermediate stream. It is worth mentioning that the volume of Sydney LGA is different in the two sets of data analysis because weekdays are 16 hours of data, while non-working days are 24 hours of data.

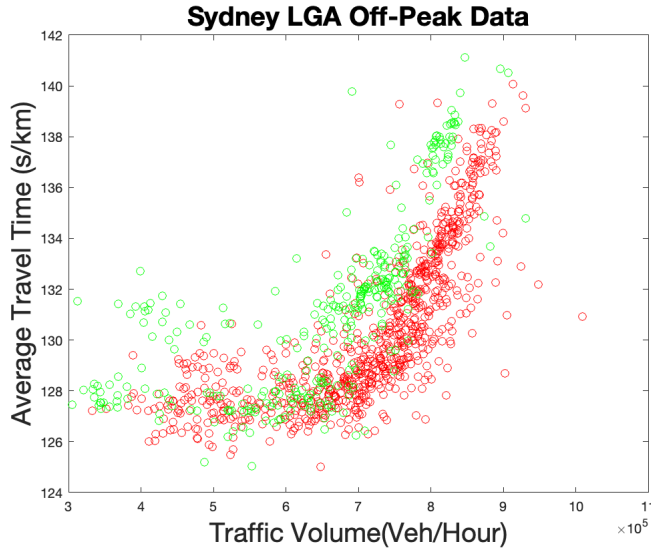


Fig. 4: Sydney LGA Off-peak Summary

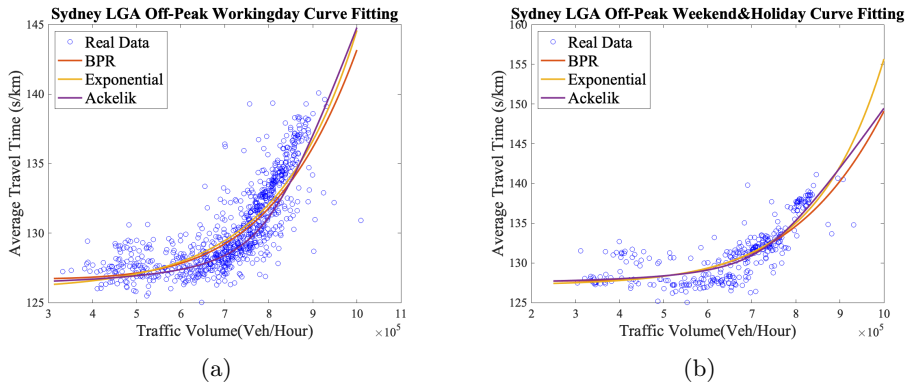


Fig. 5: Sydney LGA Off Peak Hour Fitting Results

### 5.4.3 Peak Hours in Suburb

Fig.6 summarizes the fit results in the suburban area. Fig.6(a) shows the geographic information of the three suburban areas. Fig.6(b) is a different function for Sydney suburban road data. Fig.6(c) is a separate function for the Parramatta suburban road data, and Fig.6(d) is a different function fit for the North Sydney suburban road data. Each point represents the value of the off-peak travel time for weekdays. The distribution of these data is similar to that of the LGAs. The results are also identical to those obtained in all three LGAs.

**Table 4:** Results in the Sydney LGA Off-peak Hour

Off-peak Hour	Model	Capacity (V/H)	a	b	c	$R^2$	RMSE
Working day	BPR	900000	5.526	5.26	126.7	0.6666	1.82
	Akcelik	900000	0.0463	1492	126.7	0.6668	1.809
	Exponential	900000	0.07374	4.497	125.9	0.6672	1.793
Weekend&Holiday	BPR	900000	5.01	5.048	127.7	0.6784	2.002
	Akcelik	900000	0.03381	2273	127.5	0.6795	1.990
	Exponential	900000	0.04448	4.846	127.2	0.6793	1.992

Table 5 provides detailed information on the function parameters and the suburb capacity. In the parameters, the value continues to express the travel time under ideal conditions. In the matching of the fit, it can be seen in the data of the three suburbs that the fit of the BPR and the exponential function is very similar, whereas the Akcelik function will be relatively lower than the other two functions.

**Table 5:** Results of the Suburb Peak Hour

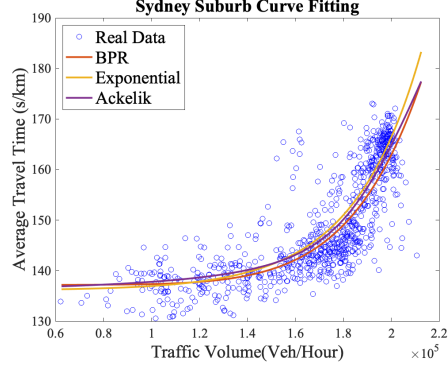
Suburb	Model	Capacity(V/H)	a	b	c	$R^2$	RMSE
Sydney	BPR	180000	15.94	7.383	137.2	0.6857	5.982
	Akcelik	180000	0.1329	592.5	136.2	0.6862	5.979
	Exponential	180000	0.0249	6.559	136.1	0.6864	5.973
Parramatta	BPR	75000	3.106	8.1	131.6	0.4501	1.714
	Akcelik	75000	0.02815	29.78	131.6	0.4452	1.772
	Exponential	75000	0.003403	6.95	131.2	0.4505	1.715
North Sydney	BPR	110000	8.682	9.426	113.5	0.6967	3.308
	Akcelik	110000	0.09292	93.04	113.6	0.6973	3.31
	Exponential	110000	0.002008	8.451	112.5	0.6974	3.305

#### 5.4.4 Summary

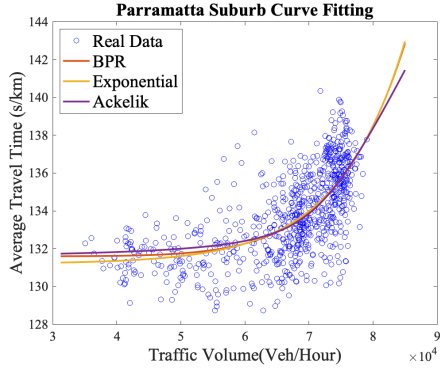
In general,  $R^2$  greater than 0.5 can be considered a moderate fit, while when  $R^2$  is greater than 0.7, the function is a stronger fit. The variance of the data can be interpreted as the data floating in a certain range. If the degree of data variance is large, it means that the data float in a wide range; on the contrary, if the degree of data variance is small, it means that the floating range is small. From the perspective of data variance, the larger the region, the smaller the dispersion of the data, while the smaller the region, the larger the data variance. This is the main reason for the large variance of the adjustment parameters. At a deeper level, large regions are more tolerant of unexpected events than small regions. For example, if a small region has a serious traffic accident, the travel time in that region will increase significantly without changing traffic. However, the average post-travel time in large regions will not change much due to the high overall traffic flow. Additionally, when comparing suburban and LGA data, it can be seen that the extent of traffic construction has a much greater impact on suburban data than on LGA data.



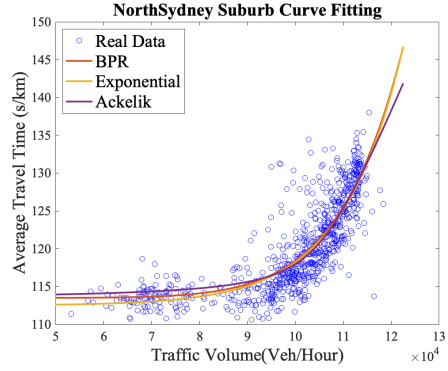
(a)



(b)



(c)



(d)

**Fig. 6: Peak Hour Results at the Suburb Level**

The data analysis shows that the exponential function has certain advantages in describing the regional cost flow function. Note that the results in this paper are fitted to data at different time intervals. To formally describe the cost flow function for the whole region, we use a split function and divide it into three parts. One of these periods is the peak time on weekdays, the second period is the off-peak time on weekdays, and the other is holidays and weekends. However, this property is derived from the fitting results of exponential functions; piecewise functions can also explain other functions. Here, we use the Sydney LGA as an example as follows.

$$t_{sydney}(x) = \begin{cases} 0.004602 \cdot e^{7.325x} + 138.5(s/km) & \text{Working day peak hour} \\ 0.07374 \cdot e^{4.497x} + 125.9(s/km) & \text{Working day non-peak hour} \\ 0.009562 \cdot e^{4.846x} + 127.2(s/km) & \text{Holiday\&weekend} \end{cases} \quad (34)$$

The above function is the Sydney LGA cost flow function with specific coefficients for different time intervals. With such data analysis, getting the travel time for different

periods is easy from a realistic perspective. If the travel time is specific to each vehicle, it must be calculated based on the distance the vehicle travels in the region. In addition, the data analysis from Sydney LGA shows that although different time intervals have different functions, the capacity of the whole region is fixed.

## 5.5 Comparing with the Upper Bound for BPR functions and Exponential Function

This section claims that the PoA is lower under realistic circumstances when roads have exponential cost functions than BPR cost functions. Each road  $p \in P$  has a **traffic capacity**  $\Phi_p \in \mathbb{R}$ , which represents the maximum number of vehicles that can pass the road in an hour, assuming “*traffic flow is not so great as to cause unreasonable delay, hazard or restriction to the driver*” (Olcott, 1955; Schleicher, Gelau, et al., 2011). This definition of traffic capacity is also known in the literature as the *practical capacity*. Here, we assume this value is the same for every road  $p$ , which we denote as  $\Phi$ . Note that, by definition of the traffic capacity, in the real world, the actual traffic flow cannot exceed the traffic capacity by much.

As explained above, the most common cost function used in the literature is the Bureau of Public Roads (BPR) function (Division, 1964), which has the form.

$$l(f) = t_0(1 + m \cdot (\frac{f}{\Phi})^n) \quad (35)$$

where  $t_0$  is free-flow travel time.

It is known from the literature, Roughgarden (2003) shows that a tight upper bound  $\hat{P}oA_{BPR}$  for the PoA over the set of all instances where the cost functions are BPR functions with the degree at most  $\hat{n}$  is given by the following:

$$\hat{P}oA_{BPR} = (1 - \hat{n}(\hat{n} + 1)^{-\frac{\hat{n}+1}{\hat{n}}})^{-1} \quad (36)$$

In the next section, we will show that if we try to model the actual cost functions of a real-world road network using the BPR function or by using exponential cost functions, then the respective values of  $\Phi$ ,  $\hat{b}$ , and  $\hat{n}$  that we get will typically satisfy  $\Phi \cdot \hat{b} \leq \hat{n}$ , which is an essential assumption for the rest of this section.

We are now ready to state our main claim in this section. A formal proof of this conjecture is left for future work.

**Conjecture 1.** *Given a road network  $G$  and any traffic demand  $\vec{r}$ , we have  $(G, \vec{r}, L_{BPR})$  and  $(G, \vec{r}, L_{exp})$ . If  $\Phi \cdot \hat{b} \leq \hat{n}$  and  $f_p^* \leq \Phi$  for all  $p \in P$  (where  $f^*$  is the equilibrium flow of the instance with exponential functions), then  $PoA(G, \vec{r}, L_{exp}) \leq \hat{P}oA_{BPR}$ .*

*Proof Idea:* We know from Lemma 3 that:

$$PoA(G, \vec{r}, L_{exp}) \leq \phi(L_{exp}) = \max_{p \in P} \phi_p(\vec{r})$$

Combining this with From Eq.(16) and Lemma 6 we get that

$$PoA(G, \vec{r}, L_{exp}) \leq \frac{\beta}{\beta + 2 - W(e^{\beta+1}) - \frac{1}{W(e^{\beta+1})}}$$

where  $\beta = \max_{p \in P} b_p f_p^*$ , and from Eq.(36) we know that

$$\hat{P}oA_{BPR} \leq (1 - \hat{n}(\hat{n} + 1)^{-\frac{\hat{n}+1}{\hat{n}}})^{-1}$$

Because of the assumption  $f_p^* \leq \Phi$  we have that  $b_p f_p^* \leq b_p \Phi$  and therefore that  $\beta \leq \hat{b} \cdot \Phi$ . Then, since we also assumed that  $\Phi \cdot \hat{b} \leq \hat{n}$  we have that  $\beta \leq \hat{n}$ . So, by Lemma 6 we have

$$\frac{\beta}{\beta + 2 - W(e^{\beta+1}) - \frac{1}{W(e^{\beta+1})}} \leq \frac{\hat{n}}{\hat{n} + 2 - W(e^{\hat{n}+1}) - \frac{1}{W(e^{\hat{n}+1})}} \quad (37)$$

We then only need to show that, for any positive  $\hat{n}$  we have

$$(1 - \hat{n}(\hat{n} + 1)^{-\frac{\hat{n}+1}{\hat{n}}})^{-1} - \frac{\hat{n}}{\hat{n} + 2 - W(e^{\hat{n}+1}) - \frac{1}{W(e^{\hat{n}+1})}} \geq 0 \quad (38)$$

Rather than formally proving this inequality, we argue that it is true by showing a plot of the left-hand side of Eq.(38). This plot is displayed in Figure 7. The graph on the left shows a range of  $\hat{n}$ -values of 0 – 10, and the graph on the right shows a range of  $\hat{n}$ -values of 0 – 100.

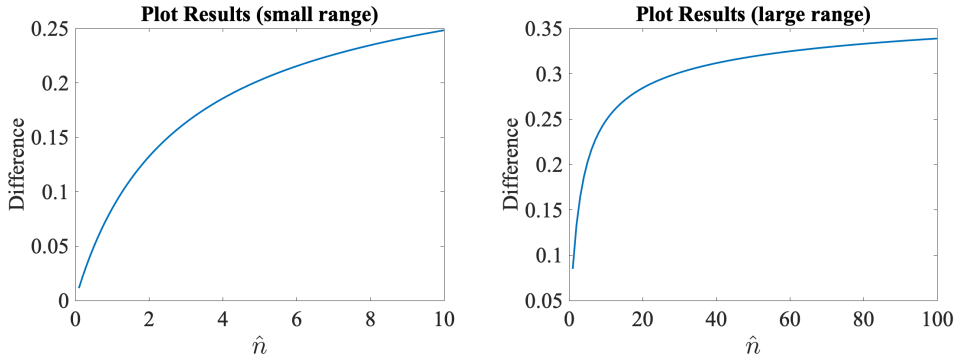


**Fig. 7:** Plot Results for Conjecture 1

Besides the conjecture, we use the function fit results obtained in section 5.4 to perform a PoA comparison between the BPR and exponential functions and show the real-world meaning of the PoA in the rest of this subsection. From the definition of anarchy value (see Def.4) and results of Lemma 3, we know that the highest anarchy value in that road network determines the upper bound of the PoA of a road network. Drawing on these results, we calculate anarchy values for the coefficients of the fit function obtained for each data region and compare them.

For BPR functions, the anarchy value of a region is calculated as  $(1 - b(b + 1)^{-\frac{b+1}{b}})^{-1}$  (Roughgarden, 2003), where  $b$  is the exponent of the polynomial function. And for exponential functions, the anarchy value of a region is calculated as  $\frac{br}{br+2-W(e^{br+1})-\frac{1}{W(e^{br+1})}}$  (See Lemma 4). We selected the results of fitting the BPR function and exponential function for the peak period data in Table 2 for different regions as the basis for the calculations in Table 6. Traffic demand are divided into four cases: Low ( $r = 0.25$ ), Medium ( $r = 0.5$ ), High ( $r = 0.75$ ), and Full ( $r = 1$ ).

**Table 6:** Anarchy Value Comparison with different traffic demand

Peak Hour	Traffic Demand	BPR	Exponential
Sydney	Low	3.10	1.45
	Medium	3.10	1.88
	High	3.10	2.30
	Full	3.10	2.70
Parramatta	Low	2.44	1.31
	Medium	2.44	1.61
	High	2.44	1.90
	Full	2.44	2.18
North Sydney	Low	3.21	1.49
	Medium	3.21	1.97
	High	3.21	2.42
	Full	3.21	2.86

The results from Table 6 show that, in general, using the exponential function instead of the BPR function as the cost function of the road network yields relatively low PoA upper bounds. This result is affected by the restrictiveness of the PoA upper bound of the BPR function, as it results from the coefficients of the function itself only. And the PoA upper bound result of the exponential function is the result of the joint action of the traffic demand and the function coefficient. Combining the combined results of the data in Lemma 6 and Table 6 shows that the anarchy value of the exponential function in a road network increases monotonically with the increase in traffic demand. In summary, the anarchy value calculated using the real data fitting exponential function corroborates Conjecture 1 from the perspective of real data when the traffic demand is lower than the capacity.

## 6 Conclusions and Future Works

Traffic assignment with selfish routing is inefficient because it generally does not achieve the optimal solution that could be achieved if all vehicles cooperated. The price of anarchy describes this inefficiency. Since the traditional approach to calculating the PoA upper bound uses different types of functions for simplification, and the results are related to only exponents, the impact of changes in traffic demand on it is not addressed.

This paper focuses on the tight upper bound price of anarchy in road networks using exponential cost functions and discusses the changes in the tight upper bound due to changes in traffic demand. For the realistic case, traffic demand cannot be much greater than capacity, so we compare the trend of PoA with traffic demand when the same road network topology's cost function is exponential or BPR function. We have used a real traffic database as support to verify the validity of the exponential cost function and found that the exponential function can provide higher accuracy compared to the BPR function. And the results show that when the traffic rate is lower than capacity, using the exponential cost function yields a tight upper bound on PoA that is lower than the BPR function.

The conjectures mentioned in this paper are not mathematically proven, and more formal theoretical proofs as an aspect of future work. Second, extending the exponential function to a broader range of application scenarios is the focus of future work. In addition, more research on PoA can be considered instead of simply considering traffic scenarios.

## References

- Aashtiani, H.Z., & Magnanti, T.L. (1981). Equilibria on a congested transportation network. *SIAM Journal on Algebraic Discrete Methods*, 2(3), 213–226,
- Akcelik, R. (1978). A new look at davidson’s travel time function. *Traffic Engineering & Control*, 19(N10), ,
- Akella, A., Seshan, S., Karp, R., Shenker, S., Papadimitriou, C. (2002). Selfish behavior and stability of the internet: A game-theoretic analysis of tcp. *ACM SIGCOMM Computer Communication Review*, 32(4), 117–130,
- Aland, S., Dumrauf, D., Gairing, M., Monien, B., Schoppmann, F. (2011). Exact price of anarchy for polynomial congestion games. *SIAM Journal on Computing*, 40(5), 1211–1233,
- Beckmann, M., McGuire, C.B., Winsten, C.B. (1956). *Studies in the economics of transportation* (Tech. Rep.).
- Carpenter, R. (1960). Principles and procedures of statistics, with special reference to the biological sciences. *The Eugenics Review*, 52(3), 172,
- Chen, A., Yang, H., Lo, H.K., Tang, W.H. (1999). A capacity related reliability for transportation networks. *Journal of advanced transportation*, 33(2), 183–200,
- Christodoulou, G., & Koutsoupias, E. (2005). The price of anarchy of finite congestion games. *Proceedings of the thirty-seventh annual acm symposium on theory of computing* (pp. 67–73).
- Cominetti, R., Dose, V., Scarsini, M. (2021). The price of anarchy in routing games as a function of the demand. *Mathematical Programming*, 1–28,
- Corless, R.M., Gonnet, G.H., Hare, D.E., Jeffrey, D.J., Knuth, D.E. (1996). On the lambertw function. *Advances in Computational mathematics*, 5(1), 329–359,

- Dafermos, S.C., & Sparrow, F.T. (1969). The traffic assignment problem for a general network. *Journal of Research of the National Bureau of Standards B*, 73(2), 91–118,
- Dheenadayalu, Y., Wolshon, B., Wilmot, C. (2004). Analysis of link capacity estimation methods for urban planning models. *Journal of transportation engineering*, 130(5), 568–575,
- Division, U.P. (1964). *Traffic assignment manual for application with a large, high speed computer*. US Department of Commerce.
- Feldman, M., Immorlica, N., Lucier, B., Roughgarden, T., Syrgkanis, V. (2016). The price of anarchy in large games. *Proceedings of the forty-eighth annual acm symposium on theory of computing* (pp. 963–976).
- Gibbons, R., et al. (1992). A primer in game theory.
- Glantz, S.A., & Slinker, B.K. (2001). *Primer of applied regression & analysis of variance*, ed. McGraw-Hill, Inc., New York.
- Hoorfar, A., & Hassani, M. (2007). Approximation of the lambert w function and hyperpower function. *Research report collection*, 10(2), ,
- Jastrzebski, W. (2000). Volume delay functions. *15th international emme/2 users group conference*.
- Johari, R., & Tsitsiklis, J.N. (2004). Efficiency loss in a network resource allocation game. *Mathematics of Operations Research*, 29(3), 407–435,
- Konishi, H. (2004). Uniqueness of user equilibrium in transportation networks with heterogeneous commuters. *Transportation science*, 38(3), 315–330,
- Koutsoupias, E., & Papadimitriou, C. (1999). Worst-case equilibria. *Annual symposium on theoretical aspects of computer science* (pp. 404–413).
- Li, R., Zhao, Z., Zhou, X., Palicot, J., Zhang, H. (2014). The prediction analysis of cellular radio access network traffic: From entropy theory to networking practice. *IEEE Communications Magazine*, 52(6), 234–240,

- Liu, H.X., He, X., He, B. (2009). Method of successive weighted averages (mswa) and self-regulated averaging schemes for solving stochastic user equilibrium problem. *Networks and Spatial Economics*, 9(4), 485–503,
- Márquez, L., García, D.E., Guarín, L.C. (2014). Conical and the bpr volume-delay functions for multilane roads in bogota. *Revista de Ingeniería*(41), 30–39,
- Milchtaich, I. (2005). Topological conditions for uniqueness of equilibrium in networks. *Mathematics of Operations Research*, 30(1), 225–244,
- Morlok, E.K., & Chang, D.J. (2004). Measuring capacity flexibility of a transportation system. *Transportation Research Part A: Policy and Practice*, 38(6), 405–420,
- Mosher Jr, W.W. (1963). A capacity-restraint algorithm for assigning flow to a transport network. *Highway Research Record*(6), ,
- Mtoi, E.T., & Moses, R. (2014). Calibration and evaluation of link congestion functions: applying intrinsic sensitivity of link speed as a practical consideration to heterogeneous facility types within urban network. *Journal of Transportation Technologies*, ,
- O’Hare, S.J., Connors, R.D., Watling, D.P. (2016). Mechanisms that govern how the price of anarchy varies with travel demand. *Transportation Research Part B: Methodological*, 84, 55–80,
- Olcott, E.S. (1955). The influence of vehicular speed and spacing on tunnel capacity. *Journal of the Operations Research Society of America*, 3(2), 147–167,
- Organization, W.H., et al. (2019). Trends in maternal mortality 2000 to 2017: estimates by who, unicef, unfpa, world bank group and the united nations population division.
- Overgaard, K.R. (1967). Urban transportation planning’traffic estimation. *Traffic Quarterly*, 21(2), ,
- Pigou, A.C., & Aslanbeigui, N. (2017). *The economics of welfare*. Routledge.

- Rosenthal, R.W. (1973). A class of games possessing pure-strategy nash equilibria. *International Journal of Game Theory*, 2(1), 65–67,
- Roughgarden, T. (2003). The price of anarchy is independent of the network topology. *Journal of Computer and System Sciences*, 67(2), 341–364,
- Roughgarden, T. (2005). *Selfish routing and the price of anarchy*. MIT press.
- Roughgarden, T., & Tardos, É. (2002a). How bad is selfish routing? *Journal of the ACM (JACM)*, 49(2), 236–259,
- Roughgarden, T., & Tardos, E. (2002b, March). How bad is selfish routing? *J. ACM*, 49(2), 236–259, <https://doi.org/10.1145/506147.506153> Retrieved from <https://doi.org/10.1145/506147.506153>
- Sandholm, W.H. (2001). Potential games with continuous player sets. *Journal of Economic theory*, 97(1), 81–108,
- Sandholm, W.H. (2010). *Population games and evolutionary dynamics*. MIT press.
- Schleicher, S., Gelau, C., et al. (2011). The influence of cruise control and adaptive cruise control on driving behaviour—a driving simulator study. *Accident Analysis & Prevention*, 43(3), 1134–1139,
- Smock, R. (1962). An iterative assignment approach to capacity restraint on arterial networks. *Highway Research Board Bulletin*(347), ,
- Soltman, T.J. (1966). Effects of alternate loading sequences on results from chicago trip distribution and assignment model. *Highway research record*(114), ,
- Spiess, H. (1990). Conical volume-delay functions. *Transportation Science*, 24(2), 153–158,
- Taylor, M. (1997). The effects of lower urban speed limits on mobility, accessibility, energy and the environment: Trade-offs within increased safety. *Transport Systems Centre, School of Geoinformatics Planning and Building, University of South Australia, Australia*. [www.infrastructure.gov.au/roads/safety/publications/1997/pdf/lower\\_urb\\_speed.pdf](http://www.infrastructure.gov.au/roads/safety/publications/1997/pdf/lower_urb_speed.pdf), ,

- Wang, X., Xiao, N., Xie, L., Frazzoli, E., Rus, D. (2015). Analysis of price of anarchy in traffic networks with heterogeneous price-sensitivity populations. *IEEE Transactions on Control Systems Technology*, 23(6), 2227-2237, <https://doi.org/10.1109/TCST.2015.2410762>
- Wardrop, J.G. (1952a). Road paper. some theoretical aspects of road traffic research. *Proceedings of the Institution of Civil Engineers*, 1(3), 325-362, <https://doi.org/10.1680/ipeds.1952.11259> Retrieved from <https://doi.org/10.1680/ipeds.1952.11259>
- Wardrop, J.G. (1952b). Road paper. some theoretical aspects of road traffic research. *Proceedings of the institution of civil engineers*, 1(3), 325-362,
- Weisstein, E.W. (2002). Lambert w-function. <https://mathworld.wolfram.com/>, ,
- Xie, Y., Zhang, Y., Ye, Z. (2007). Short-term traffic volume forecasting using kalman filter with discrete wavelet decomposition. *Computer-Aided Civil and Infrastructure Engineering*, 22(5), 326-334,
- Zhang, J., Pourazarm, S., Cassandras, C.G., Paschalidis, I.C. (2016). The price of anarchy in transportation networks by estimating user cost functions from actual traffic data. *2016 IEEE 55th conference on decision and control (cdc)* (pp. 789-794).
- Zhang, J., Pourazarm, S., Cassandras, C.G., Paschalidis, I.C. (2018). The price of anarchy in transportation networks: Data-driven evaluation and reduction strategies. *Proceedings of the IEEE*, 106(4), 538-553,